DOI: 10.1002/ejoc.200800905

Diverse and Yet Unified: A Comparative Study of the Supramolecular Assemblies of Three Diastereomeric Perhydro-2,3,4a,6,7,8a-naphthalenehexols

Goverdhan Mehta*[a] and Saikat Sen[a]

Keywords: Chirality / Hydrogen bonds / Supramolecular chemistry / Conformational locking

Self-assemblies of three crystalline perhydro-2,3,4a,6,7,8a-naphthalenehexols **3**–**5**, all constructed on a *trans*-decalin framework, were compared with each other and to that of their diastereomeric *all axial* hydroxy sibling **2**, which was previously reported. The presence of the peripheral equatorial OH groups in **3**–**5** severs, to varying extents, the end-to-end intramolecular O–H···O hydrogen-bonding chain linking the 1,3-diaxial hydroxy groups on both faces of hexol **2**. Hence, the crystal packing in **3**–**5** deviates from the simple qualitative model proposed and observed in **2**. Though complex and seemingly individualistic upon a cursory glance, the supramolecular assemblies of all three hexols underscore two primary concepts of O–H···O hydrogen bonding, namely, maximization of the total number of hydrogen bonds per molecule and maximization of O–H···O hydrogen-bond cooperativity by forming as many finite and infinite chains of hydrogen bonds as possible.

Introduction

With only one functional group, namely, the hydroxy group, functioning as both donor and acceptor of hydrogen bonds in the molecule, polyols, such as carbohydrates and inositols, have constituted one of the earliest and simplest systems for the analysis of O–H···O hydrogen bonding.[1] However, in most cases, logical anticipation of the mode of molecular association in such molecules becomes a difficult proposition owing to the orientational flexibility of the C–OH groups.[1c] Proposing the hydrogen-bonded architecture in polyols, with little or no constraints to the internal degrees of freedom, proves to be even more complicated, as the final spatial disposition of the hydroxy groups, realized in the crystal structure of such molecules, is often largely determined by the crystal packing itself.

Against this background, we have been actively involved, for quite some time now, in the pursuit of elucidating the patterns of self-assembly in conformationally locked polycyclitols, specially crafted on a rigid *trans*-decalin carbocyclic backbone **1** in order to obtain a ground-state *axial rich* disposition of the hydroxy groups.[2] As a part of this ongoing research, we recently reported the crystal packing in bicyclic, C_{2h}-symmetric hexol **2**, having a novel *all axial* disposition of the six hydroxy functionalities.[2d] Intramolecular H-bonding between the 1,3-diaxial OH groups in **2** preordained the positions of the intermolecular O–H···O hydrogen-bond donors and acceptors, which not only simplified a qualitative visualization of the various packing patterns in **2**, but also allowed us to propose, on the basis of previously reported CSD analyses, the packing motifs most likely to converge with the experimental results (Figure 1). Albeit qualitative in nature, the O–H···O hydrogen-bonding pattern proposed for **2** was found to conform well with that observed experimentally for the two observed polymorphs of hexol **2**.[2d,2e]

1 (conformationally locked 9,10-*trans*-dihydroxydecalin)

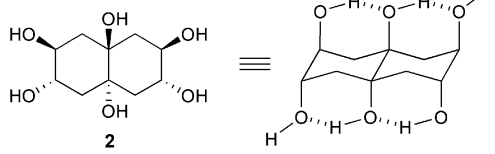

2

The deterministic role played by intramolecular O–H···O hydrogen bonding in the supramolecular assembly of **2** prompted us to study the crystal packing of diastereomeric perhydro-2,3,4a,6,7,8a-naphthalenehexols **3**–**5**, all conformationally locked like **2** owing to their elaboration on a *trans*-decalin scaffold. Polyols **3**–**5** were conceptualized with the intent of severing the end-to-end cooperative intramolecular O–H···O–H hydrogen-bonding chain on both faces of the molecule, as observed in **2**, through an axial–equatorial transposition of one or more of the peripheral hydroxy groups (Figure 2). With increased freedom now allowed to

[a] Department of Organic Chemistry, Indian Institute of Science, Bangalore 560012, India
Fax: +91-80-23600283
E-mail: gm@orgchem.iisc.ernet.in

Supporting information for this article is available on the WWW under http://www.eurjoc.org or from the author.

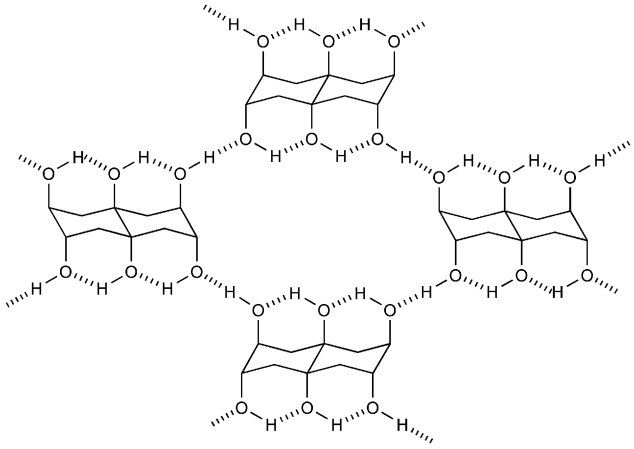

Figure 1. One of the packing modes proposed and observed experimentally for hexol **2**. Note that the H-bonding pattern involves all donor/acceptor oxygen atoms and incorporates infinite chains of O–H···O bonds.

the OH groups in the choice of their H-bonding partners, in comparison to **2**, crystal packing in polycyclitols **3**–**5** was expected to evolve from the simplistic model of hydrogen bonding proposed and observed for **2** to invoke more complex patterns of self-assembly mediated through O–H···O hydrogen bonds (Figure 1). In this context, the present study analyzes the extent to which the supramolecular assemblies of isomeric hexols **3**–**5** correlate with or differ from each other.

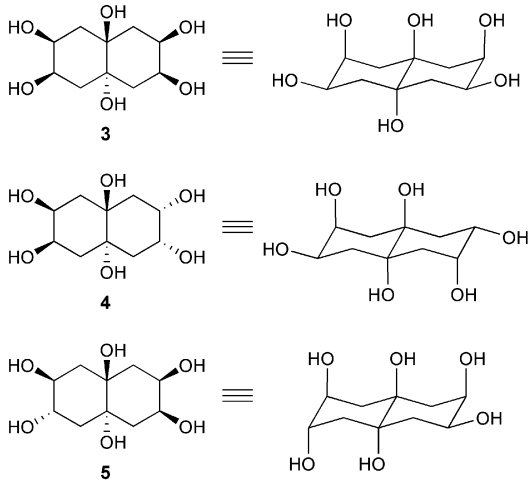

Results and Discussion

Synthesis of Isomeric Hexols 3–5

Synthesis of C_s-symmetric hexol **3** commenced from *trans*-diol **6**, conveniently prepared from Birch reduction product **7** of naphthalene according to an earlier reported procedure.[4] Catalytic OsO_4 mediated exhaustive dihydroxylation of **6** furnished **3**, which was isolated from the reaction mixture as tetraacetate **8**. Exposure of **8** to K_2CO_3/MeOH gave hexol **3** in quantitative yield (Scheme 1). Though tlc and spectroscopic means of characterization pointed towards hexol **3** being the sole product of the dihydroxylation step, a miniscule amount (<0.01 mg) of isomeric hexol **4** could be isolated as a sole crystal from one of the crystallization batches of **3**, carried out on a 25-mg scale.[5]

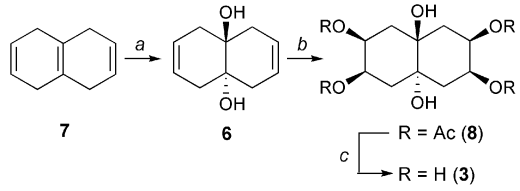

Scheme 1. Reagents and conditions: (a) Ref.[4]; (b) (i) OsO_4 (5 mol-%), NMMO, acetone/water (4:1), room temp., 8 h; (ii) Ac_2O, DMAP, room temp., 6 h, 60% over two steps; (c) K_2CO_3, MeOH, room temp., 5 h, quant. [Note: a trace amount of hexol **4** was also formed during the dihydroxylation step].[5]

syn-Diol **9**, obtained upon regioselective dihydroxylation of **7** at low temperature, formed the starting material for the synthesis of hexol **5**.[6] Exhaustive epoxidation of **9** with *m*-CPBA, followed by mild acid-catalyzed ring opening in the mixture of diepoxides thus obtained, afforded **5** as a single diastereomer. In order to facilitate purification of polar hexol **5**, the latter was first converted into tetraacetate

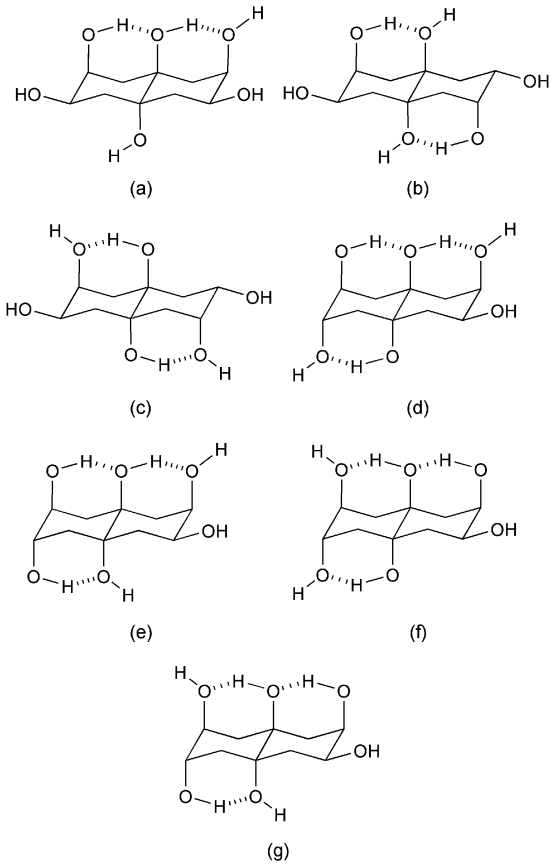

Figure 2. Modes of intramolecular O–H···O hydrogen bonding most likely to be observed in hexols **3** (a), **4** (b) and (c), and **5** (d–g). In proposing the H-bonding patterns (b) and (c), it was assumed that C_i-symmetric hexol **4** occupies a crystallographic inversion center.[2d,3]

10, from which polyol **5** was regenerated almost quantitatively through base-catalyzed transesterification (Scheme 2).[5b]

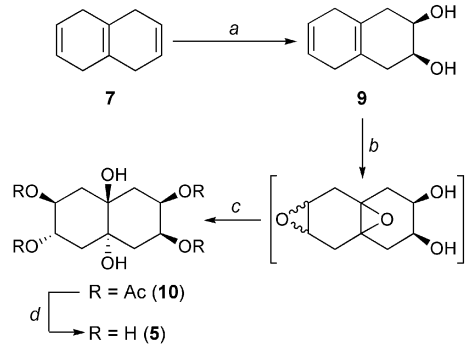

Scheme 2. Reagents and conditions: (a) Ref.[6]; (b) *m*-CPBA, CH_2Cl_2, room temp., 3 h; (c) (i) 10% AcOH (aq.), 55 °C, 4 h; (ii) Ac_2O, DMAP, room temp., 6 h, 75% over steps (b) and (c); (d) K_2CO_3, MeOH, room temp., 6 h, quant.

X-ray Crystallographic Studies on Hexols 3–5

Crystals of isomeric hexols **3** and **5**, suitable for single-crystal X-ray crystallography, were grown under ambient temperature and pressure from their solutions in methanol/ethyl acetate (1:1) by slow solvent evaporation. As described in the preceding section, a tiny block-like single crystal of hexol **4** was obtained in one of the crystallization batches of **3**, and it was used in toto for the X-ray diffraction studies. The details of the packing patterns in polycyclitols **3**–**5**, as gleaned from analysis of their respective crystal data (see Table 4), are discussed below.

Crystal Structure of Hexol 3

Achiral, C_s-symmetric hexol **3** packed in the chiral orthorhombic space group $P2_12_12_1$ ($Z = 8$).[7] The 1,3-diaxial hydroxy groups in both of the two symmetry independent hexol molecules (arbitrarily designated as A and B) in the asymmetric unit participate in intramolecular O–H···O hydrogen bonding (Figures 2a and 3). Intermolecular O–H···O hydrogen bonding, involving O1···O11 (A→B), O11···O3 (B→A), O12···O2 (B→A), and O7···O8 (B→B), link the hexol molecules in a ···B→B→A→B→B→A→B··· arrangement to form helical molecular chains, growing essentially parallel to the longest *c* axis (Figure 4). The helices, translated along the *a* axis, are further connected by hydrogen bonds involving O5···O2 (A→A), O2···O6 (A→A), and O8···O12 (B→B) to form H-bonded tapes. These molecular tapes then interconnect with each other along the *b* axis through the intermediacy of a "connector" A molecule with O6···O4 hydrogen bonds to generate an intricate three-dimensional supramolecular assembly (Figure 5, Table 1). Interestingly, an alternate tracing of the O–H···O hydrogen bond connectivity between the helices along the *b* axis reveal, as shown in Figure 6, a complex intertwined double helical self-assembly of the hexol molecules.

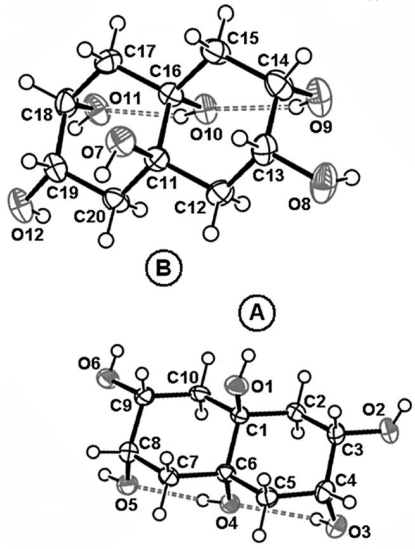

Figure 3. ORTEP diagram of hexol **3**, with the atom numbering scheme for the asymmetric unit. Displacement ellipsoids are drawn at the 50% probability level, and H atoms are shown as small spheres of arbitrary radii. The grey dotted lines indicate the intramolecular O–H···O hydrogen bonds.

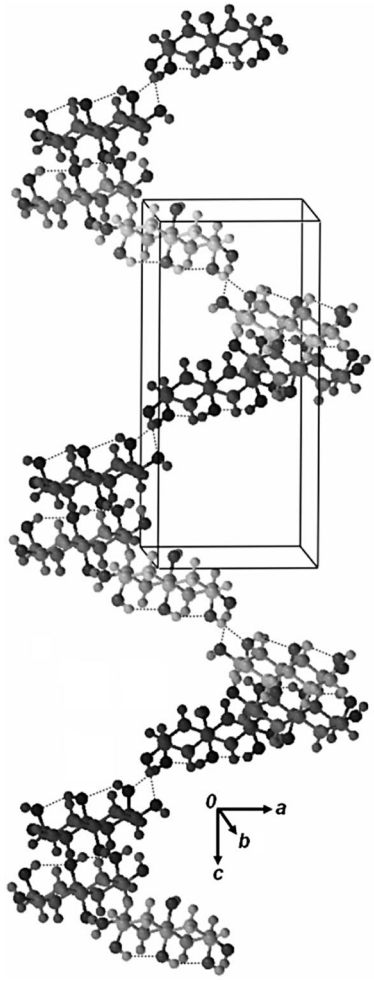

Figure 4. Ball-and-stick representation of the molecular packing in hexol **3**, showing details of the helical self-assembly mediated by O–H···O hydrogen bonds.

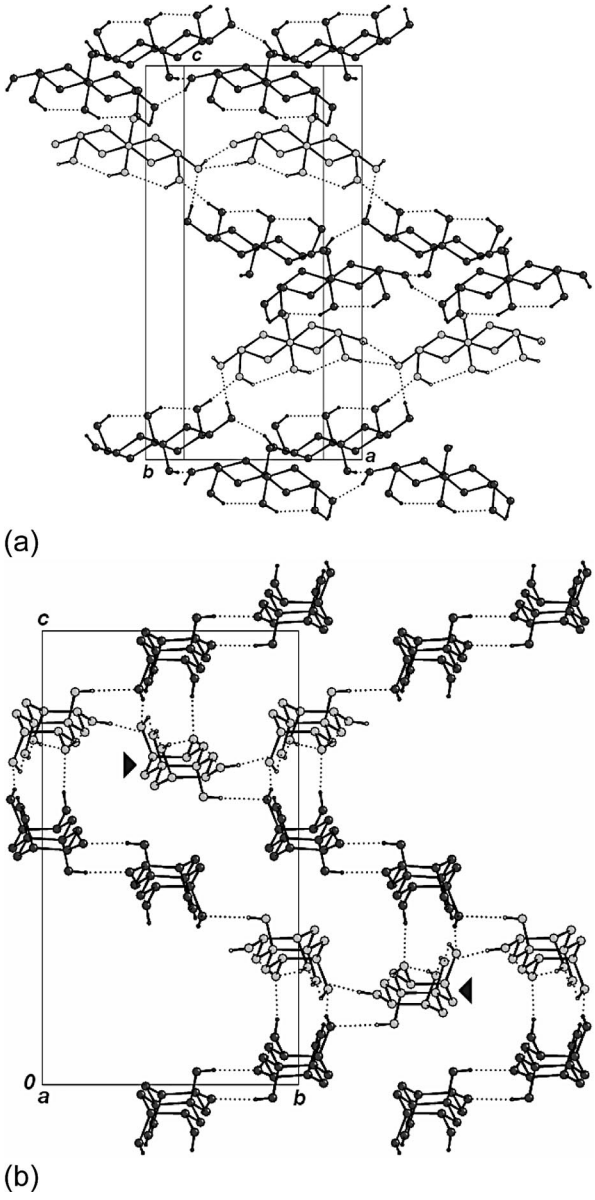

Figure 5. Molecular packing in hexol **3**, showing details of the O–H···O hydrogen-bonding interconnectivity between the helical strands, translated along (a) the *a* axis and (b) the *b* axis. In both figures, the constituent A and B molecules of each helix are colored in light and dark shades of grey respectively. In (b), the arrows indicate the "connector A molecules", linking the helices along the *b* axis. H atoms bonded to C atoms are omitted for the sake of clarity.

A novel feature of the molecular packing in crystalline **3** should be noted at this point. It is well known that achiral molecules prefer to crystallize in centrosymmetric space groups.[9] In this context, the supramolecular assembly of hexol **3** is reminiscent of that observed in quartz and γ-glycine,[10] wherein the chirality of the crystal is derived from the handedness of the helical assembly of the molecules.[1a,11] Although it is difficult to provide the raison d'être for the chiral molecular packing of hexol **3**, a clue can still be gleaned from the CSD analysis, carried out by Pidcock on the structural determinants of space group pref-

Table 1. Hydrogen bond geometry in hexol **3**.[a]

D–H···A	D–H [Å]	H···A [Å]	D···A [Å]	D–H···A [°]
O1–H1O···O11^{i}	0.82	2.11	2.928(3)	172
O2–H2O···O6^{ii}	0.82	1.91	2.684(3)	158
O3–H3O···O4^{iii}	0.82	2.26	2.827(3)	127
O4–H4O···O5^{iii}	0.82	1.99	2.703(3)	145
O5–H5O···O2^{iv}	0.82	2.12	2.929(3)	171
O6–H6O···O4^{v}	0.82	2.00	2.806(3)	170
O7–H7O···O8^{vi}	0.82	2.01	2.817(3)	170
O8–H8O···O12^{ii}	0.82	1.92	2.655(3)	149
O9–H9O···O10^{iii}	0.82	2.04	2.736(3)	142
O10–H10O···O11^{iii}	0.82	1.97	2.695(3)	147
O11–H11O···O3^{vii}	0.82	1.96	2.755(3)	165
O12–H12O···O2^{vii}	0.82	1.96	2.766(3)	170

[a] Symmetry codes: (i) $-x + 3/2, -y + 1, z - 1/2$; (ii) $x - 1, y, z$; (iii) x, y, z; (iv) $x + 1, y, z$; (v) $-x + 2, y - 1/2, -z + 1/2$; (vi) $x + 1/2, -y + 3/2, -z + 2$; (vii) $x + 1/2, -y + 3/2, -z + 1$.

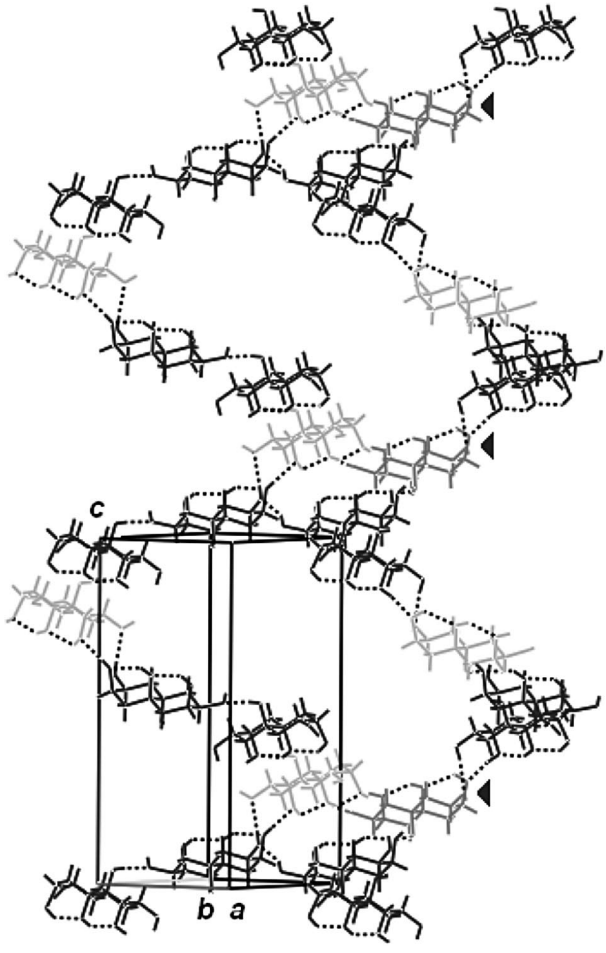

Figure 6. An intertwined double-helical self-assembly, identified through an alternate tracing of the O–H···O hydrogen bond connectivity in the crystal structure of hexol **3**. Color coding of the A and B molecules follows from that of Figure 5. The "connector A molecules" are darkened slightly and indicated by arrows. Notice that the intermolecular O–H···O hydrogen bonds in the helical strand on the left thread through the "connector A molecules" and follow an antiparallel sense in their sequence to those present in the right helix.

erences in achiral molecules.[12] The study had concluded that conformationally rigid molecules, particularly those like **3**, possessing a mirror symmetry, exhibit an increased propensity to crystallize in a chiral space group, possibly on account of the equivalence of an inversion operation, carried out on a C_s symmetric molecule, to a rotation symmetry. Although it is interesting to note that hexol **3** subscribes to the choice of space group laid down in the aforesaid CSD analysis, an alternate explanation to the chirality in the solid-state supramolecular assembly of **3** also exists. The crystal structure of **3** would have been centrosymmetric if the translated helical chains, built of molecules following the 2_1 symmetry parallel to the *a* and *c* axes, ran antiparallel to each other. However, the helical chains, translated along the [010] direction, are also threaded through by A molecules that follow the 2_1 symmetry parallel to the *b* axis (a symmetry operation arising from the combination of 2_1 symmetry parallel to the *a* and *c* axes; Figure 5b). This results in a transmission of polarity among the translationally related helical chains and eventually culminates in the chiral molecular self-assembly of hexol **3**.

Crystal Structure of the Hemihydrate of Hexol 4

C_i-symmetric hexol **4** crystallized as a hemihydrate in the centrosymmetric monoclinic space group *C*2/*c* (*Z* = 4). Analysis of the crystal structure revealed that the asymmetric unit contains two symmetry independent hexol mole-

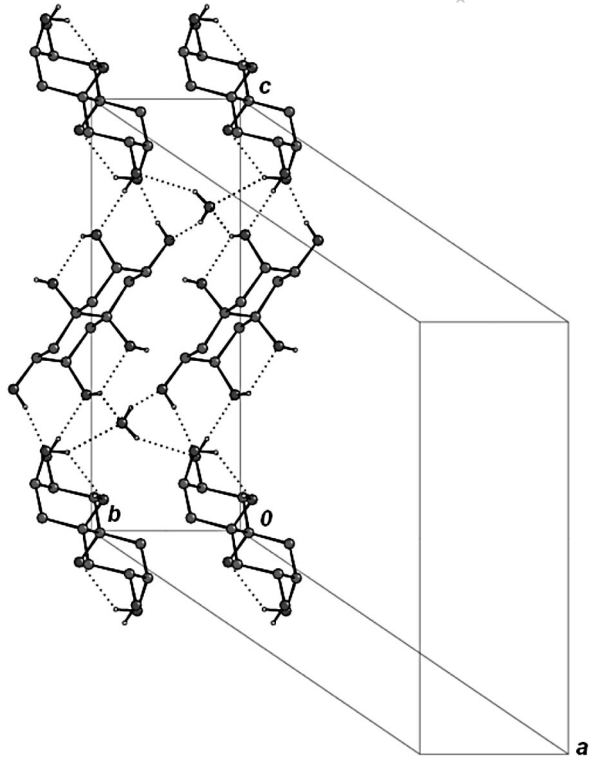

Figure 8. Molecular packing in the hemihydrate of hexol **4**, showing details of the O–H···O hydrogen-bond interconnectivity in the hydrated layers of B molecules.

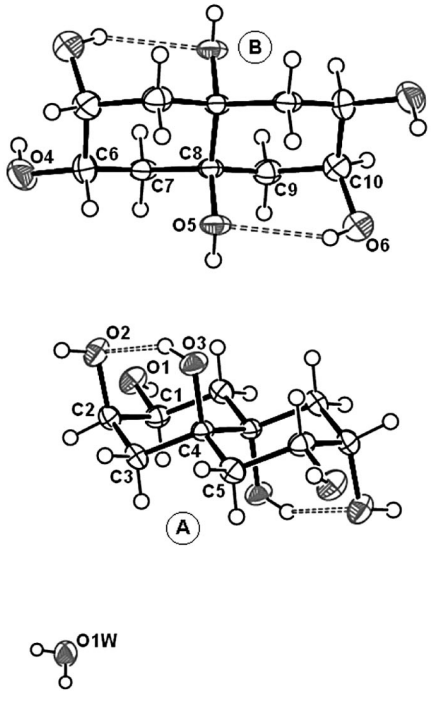

Figure 7. ORTEP diagram of the hemihydrate of hexol **4**, with the atom numbering scheme for the asymmetric unit. Displacement ellipsoids are drawn at the 50% probability level, and H atoms are shown as small spheres of arbitrary radii. The grey dotted lines indicate the intramolecular O–H···O hydrogen bonds.

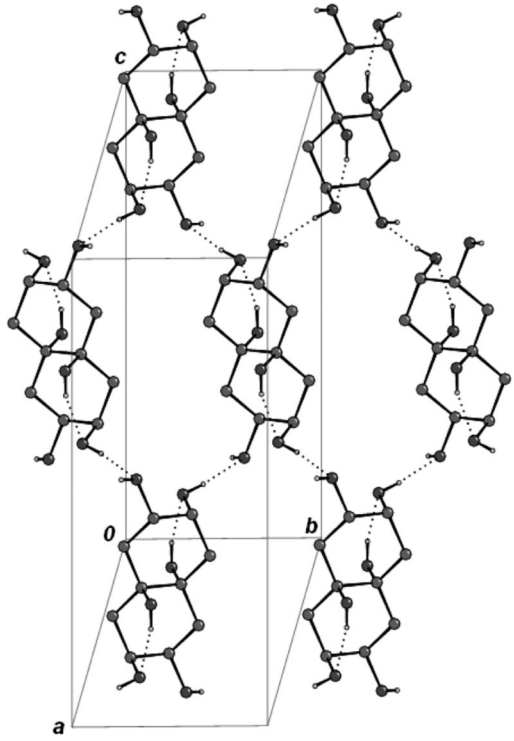

Figure 9. Molecular packing in the hemihydrate of hexol 4, showing details of the O–H···O hydrogen-bond interconnectivity in the layers of A molecules.

cules (designated arbitrarily as A and B), occupying the inversion centers at (0.25, 0.25, 0) and (0, 0, 0), respectively, and a molecule of water lying on the twofold axis passing through (0, 0 0.75; Figure 7). As seen in its sibling **3**, the 1,3-diaxial hydroxy groups of hexol **4** participate in intramolecular O–H···O hydrogen bonding, and the A and B molecules correspond to the H-bonded molecular motifs represented by Figure 2c,b. Each water molecule in the supramolecular assembly of **4** exhibits a near tetrahedral coordination around the oxygen atom, and is linked to four B molecules through O–H···O hydrogen bonds, involving the axial O6 acting as the H-bond donor and the equatorial O4 acting as the H bond acceptor. The vicinal hydroxy groups of the B molecules link to each other through intermolecular O–H···O hydrogen bonds in a commonly encountered $R^2_2(10)$ dimeric motif[13] to form wave-like molecular tapes, growing parallel to the *c* axis (Figure 8). Sandwiched between and interconnecting the H-bonded tapes of B molecules translated along the *a* axis, through hydrogen bonds involving O1···O4 and O5···O3, are the A molecules. The A molecules are also H-bonded (O2···O1) to each other to exhibit a centrosymmetric tetrameric arrangement of the hexol molecules, reminiscent of that observed in **2** (Figures 9 and 10, Table 2). The self-assembly of hexol **4** thus exhibits *self complexation*, wherein layers of A molecules are sandwiched between and H-bonded to hydrated layers of B molecules.

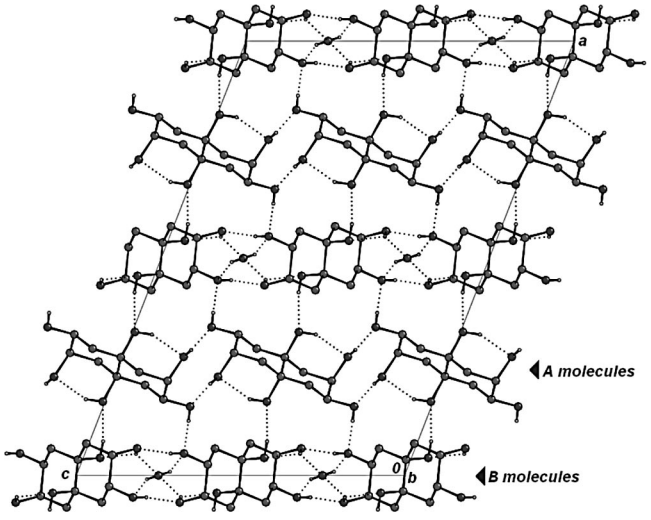

Figure 10. Self complexation in the hemihydrate of hexol **4**. Note the layers of A molecules sandwiched between layers of hydrated B molecules.

Table 2. Hydrogen-bond geometry in the hemihydrate of hexol **4**.[a]

D–H···A	D–H [Å]	H···A [Å]	D···A [Å]	D–H···A [°]
O1–H1O···O4^{i}	0.82	1.93	2.745(3)	178
O2–H2O···O1^{ii}	0.82	1.94	2.749(3)	168
O3–H3O···O2^{iii}	0.82	1.92	2.665(3)	150
O4–H4O···O6^{iv}	0.82	1.94	2.757(4)	171
O5–H5O···O3^{iii}	0.82	1.97	2.784(3)	169
O6–H6O···O1W^{v,vi}	0.82	2.26	2.976(4)	146
O1W–H1W···O4^{vii}	0.78(5)	2.27(5)	2.982(4)	152(4)

[a] Symmetry codes: (i) $-x + 1/2, y - 1/2, -z + 1/2$; (ii) $-x + 1/2, y + 1/2, -z + 1/2$; (iii) x, y, z; (iv) $x, -y, z + 1/2$; (v) $x - 1, y, z - 1$; (vi) $-x + 1, y, -z + 1/2$; (vii) $-x + 1, -y + 1, -z + 1$.

Crystal Structure of Hexol 5

The crystal structure of hexol **5** was solved and refined in the centrosymmetric monoclinic space group $P2_1/n$ ($Z = 8$) (Figure 11). The 1,3-diaxial hydroxy groups in both of

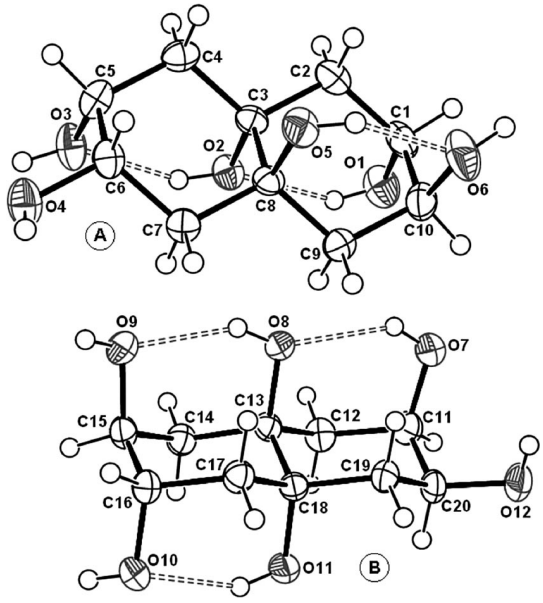

Figure 11. ORTEP diagram of hexol **5**, with the atom numbering scheme for the asymmetric unit. Displacement ellipsoids are drawn at the 50% probability level, and H atoms are shown as small spheres of arbitrary radii. The grey dotted lines indicate the intramolecular O–H···O hydrogen bonds.

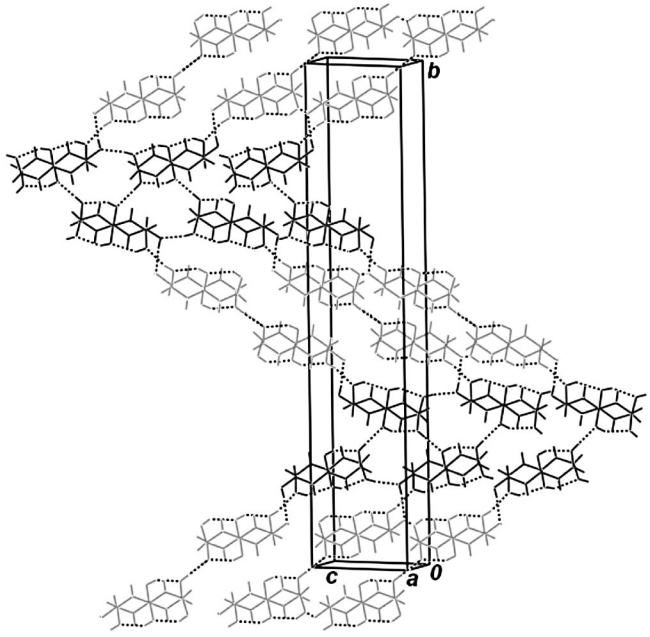

Figure 12. Molecular packing in hexol **5**. The A and B molecules are colored in light and dark shades of grey, respectively.

the two symmetry independent hexol molecules in the asymmetric unit, arbitrarily designated as A and B, participate in intramolecular O–H···O hydrogen bonding and exhibit the H-bonding patterns depicted in Figure 2d,f. Intermolecular O–H···O hydrogen bonding, involving O3···O7 (A→B), O6···O6 (A→A), O10···O11 (B→B), and O12···O4 (B→A), link the hexol molecules in a ···B→B→A→A→B→B··· arrangement to form zigzag tapes, growing essentially parallel to the longest *b* axis. The molecular tapes, translated along the [101] direction, are linked through H-bonds involving O9···O12 and O10···O11 to form sheets, which are in turn hydrogen bonded (O4···O1) along the *c* axis (Figure 12, Table 3).

Table 3. Hydrogen bond geometry in hexol **5**.[a]

D–H···A	D–H [Å]	H···A [Å]	D···A [Å]	D–H···A [°]
O1–H1O···O2^{i}	0.82	1.98	2.670(2)	141
O2–H2O···O3^{i}	0.82	1.90	2.629(2)	158
O3–H3O···O74^{ii}	0.82	1.95	2.734(2)	161
O4–H4O···O1^{iii}	0.82	1.93	2.741(3)	174
O5–H5O···O6^{i}	0.82	1.88	2.625(3)	171
O6–H6O···O6^{iv}	0.82	2.04	2.738(2)	143
O7–H7O···O8^{i}	0.82	2.08	2.768(2)	141
O8–H8O···O9^{i}	0.82	1.97	2.701(2)	147
O9–H9O···O12^{ii}	0.82	1.93	2.740(2)	169
O10–H10O···O11^{iii}	0.82	1.95	2.765(2)	178
O11–H11O···O7^{i}	0.82	1.92	2.656(2)	148
O12–H12O···O4^{vi}	0.82	1.95	2.764(3)	172

[a] Symmetry codes: (i) *x*, *y*, *z*; (ii) *x* – 1, *y*, *z* – 1; (iii) *x*, *y*, *z* – 1; (iv) –*x* + 2, –*y*, –*z* + 2; (v) *x* – 1/2, –*y* + 1/2, *z* – 1/2; (vi) *x* + 1, *y*, *z* + 1.

Concluding Remarks

The present study compares the modes of self-assembly in hexols **3**–**5**, all of which are formally diastereomers of perhydro-2,3,4a,6,7,8a-naphthalenehexol, constructed on a conformationally locked *trans*-decalin scaffold. On a cursory glance, each hexol would appear individualistic, differing from its siblings in the pattern of O–H···O hydrogen bonding and complexity of its crystal packing. However, upon closer analysis, two salient features of commonality emerge in the self-assemblies of the three hexols under study, namely, (a) maximization of the total number of hydrogen bonds per molecule by using as many donor/acceptor oxygen atoms as possible and (b) maximization of cooperativity by forming as many finite and infinite chains of hydrogen bonds as possible. These two general concepts of O–H···O hydrogen bonding, proposed by Jeffrey and Saenger for carbohydrates, were in fact at the crux of our arguments in proposing the pattern of hydrogen bonding, most likely to be observed in the crystal structure of **2**.[1c,2d] The fact that the asymmetric unit of all three hexols under study contains two symmetry independent molecules should also be noted and compared with the crystal structure of **2** in which $Z' = 1/2$. It is likely that the awkward shape of hexols **3**–**5**, resulting from the "bumps" created by the equatorial hydroxy groups, prevent the molecules from adopting a simple packing mode.[14]

To summarize, the results on the self-assembly of three conformationally locked polycyclitols, crafted through axial–equatorial transposition of hydroxy groups, clearly establish that supramolecular assemblies can evolve along separate paths on account of subtle stereochemical variation in their hydroxylation pattern while still conforming to the core concepts of H-bonding, identified in the crystal structures of alcohols and sugars. In addition to advancing the understanding of the modalities of molecular packing mediated through O–H···O hydrogen bonding, the present study also points to the importance of crystal structures of "locked" polycyclitols as promising leads for the identification of novel supramolecular synthons.

Experimental Section

Synthesis of Hexol 3: To a solution of *trans*-diol **6** (200 mg, 1.205 mmol) in acetone/water (4:1, 2 mL) was added a catalytic amount of solid osmium tetroxide (15 mg, 5 mol-%), followed by 4-methylmorpholine *N*-oxide (50 wt.-% in water, 0.850 mL, 3.614 mmol). The resulting solution was allowed to stir at ambient temperature for 8 h, after which the reaction was quenched by the addition of solid sodium bisulfite (600 mg). The mixture was then diluted with acetone to precipitate the inorganic salts, and filtered through a short pad of Celite. After washing the filter bed thoroughly with acetone, the combined filtrate and washings were concentrated under reduced pressure to obtain crude hexol **2** as a gummy mass. Compound **2** underwent acetylation in the presence of acetic anhydride (1 mL) and 4-dimethylaminopyridine (600 mg) at ambient temperature. After completion of the reaction (about 6 h as indicated by tlc), the solution was cooled in an ice bath and carefully diluted with methanol (2 mL). The volatiles were removed under reduced pressure, and the crude solid thus obtained was purified by column chromatography (65% ethyl acetate/petroleum ether) to afford tetraacetate **8** (290 mg, 60%). IR (thin film): $\tilde{\nu}$ = 3460, 1732 cm^{-1}. ^{1}H NMR (300 MHz, $CDCl_3$): δ = 5.39–5.14 (m, 4 H), 2.35 (dd appearing as a triplet, J = 12 Hz, 2 H), 2.13 (s, 6 H), 2.05–1.98 (m, 8 H), 1.86 (d, J = 16 Hz, 2 H), 1.64 (dd, J = 13, 5 Hz, 2 H) ppm. ^{13}C NMR (75 MHz, $CDCl_3$): δ = 170.6 (2 C), 169.9 (2 C), 75.3, 70.9, 69.3 (2 C), 68.3 (2 C), 35.1 (2 C), 34.4 (2 C), 21.2 (2 C), 21.0 (2 C) ppm. LRMS (ES, 70 eV): *m*/*z* = 425 [M + Na]$^{+}$. HRMS (ES): calcd. for $C_{18}H_{26}O_{10}Na$ [M + Na]$^{+}$ 425.1424; found 425.1413.

To a solution of pure tetraacetate **8** (150 mg, 0.373 mmol) thus obtained dissolved in dry methanol (1 mL) was added solid potassium carbonate (206 mg, 1.493 mmol). The reaction mixture was allowed to stir at room temperature for 5 h. The solvent was then removed completely under vacuum, and the residue was dissolved in a minimum amount of deionized water. The aqueous solution was passed through a short column of pretreated DOWEX®50W×8–200 ion-exchange resin (acidic cation) and washed with deionized water. The aqueous solution of the product thus obtained was concentrated under vacuum to obtain hexol **3** (87 mg) in quantitative yield. M.p. 232.8–233.3 °C. IR (KBr disc): $\tilde{\nu}$ = 3390 cm^{-1}. ^{1}H NMR (300 MHz, D_2O): δ = 3.87–3.84 (m, 4 H), 1.92 (dd appearing as a triplet, J = 13 Hz, 2 H), 1.83–1.52 (m, 4 H), 1.46 (dd, J = 13, 4 Hz, 2 H) ppm. ^{13}C NMR (75 MHz, D_2O): δ = 76.3, 74.3, 70.9 (2 C), 67.9 (2 C), 36.5 (2 C), 36.4 (2 C) ppm. LRMS (ES, 70 eV): *m*/*z* = 257 [M + Na]$^{+}$. HRMS (ES): calcd. for $C_{10}H_{18}O_6Na$ [M + Na]$^{+}$ 257.1001; found 257.0998.

Synthesis of Hexol 5: *syn*-Diol **9** (300 mg, 1.807 mmol) was treated at ambient temperature with *m*-CPBA (980 mg, 3.976 mmol, 70%

purity) in dry dichloromethane (4 mL) for 3 h. The reaction was then quenched by the addition of saturated aqueous sodium bisulfite solution. The product was extracted with dichloromethane (3 × 30 mL); the combined extracts were washed successively with saturated sodium hydrogen carbonate solution and brine and then dried with anhydrous sodium sulfate. Removal of the solvent afforded a crude mixture of diepoxides, which was used directly for acid-catalyzed ring opening with aqueous acetic acid (10% v/v, 4 mL) at 55 °C. After complete consumption of the staring material (about 4 h as indicated by tlc), the solvent was removed under reduced pressure to furnish crude hexol **5** as a sticky gum. To hexol **5** was added acetic anhydride (2 mL), followed by 4-dimethylaminopyridine (883 mg), and the resulting solution was allowed to stir at ambient temperature for 6 h. The reaction mixture was then cooled in an ice bath and carefully diluted with methanol (2 mL). The volatiles were removed under reduced pressure, and the crude solid thus obtained was purified by column chromatography (50% ethyl acetate/petroleum ether) to afford tetraacetate **10** (545 mg, 75%). ^{1}H NMR (300 MHz, $CDCl_3$): δ = 5.49 (d, J = 3 Hz, 1 H), 5.35 (ddd, J = 12, 4, 4 Hz, 1 H), 5.16 (br. s, 1 H), 4.99 (br. s, 1 H), 3.38 (s, 1 H), 3.22 (s, 1 H), 2.48 (dd, J = 14, 4 Hz, 1 H), 2.22–1.64 (m, 19 H) ppm. ^{13}C NMR (75 MHz, $CDCl_3$): δ = 170.0, 169.6, 169.3, 168.4, 73.6, 71.6, 70.1, 69.9, 69.1, 68.0, 35.6, 33.8, 32.8, 32.0, 21.2, 21.1, 20.9 ppm. LRMS (ES, 70 eV): m/z = 425 [M + Na]$^+$. HRMS (ES): calcd. for $C_{18}H_{26}O_{10}Na$ [M + Na]$^+$ 425.1424; found 425.1418.

Pure tetraacetate **10** (200 mg, 0.498 mmol) was taken up in dry methanol (2 mL) and stirred at ambient temperature with solid potassium carbonate (275 mg, 1.990 mmol) for 6 h. The solvent was then removed completely under vacuum, and the residue was dissolved in a minimum amount of deionized water. The aqueous solution was passed through a short column of pretreated DOWEX®50W×8–200 ion-exchange resin (acidic cation) and washed with deionized water. The aqueous solution of the product thus obtained was concentrated under vacuum to obtain hexol **5** (116 mg) in quantitative yield. IR (KBr disc): $\tilde{\nu}$ = 3390 cm^{-1}. ^{1}H NMR (300 MHz, D_2O): δ = 3.89–3.85 (m, 4 H), 2.11 (dd, J = 15, 2 Hz, 2 H), 1.91–1.46 (m, 7 H) ppm. ^{13}C NMR (75 MHz, D_2O): δ = 76.0, 75.0, 70.8, 70.7, 67.4, 36.7, 35.9, 33.4, 32.7 ppm. LRMS (ES, 70 eV): m/z = 257 [M + Na]$^+$. HRMS (ES): calcd. for $C_{10}H_{18}O_6Na$ [M + Na]$^+$ 257.1001; found 257.1006.

Crystal Structure Analysis: Single crystal X-ray diffraction data were collected with a Bruker AXS SMART APEX CCD diffractometer at 291 K. The X-ray generator was operated at 50 KV and 35 mA by using Mo-K_α radiation. The data was collected with a ω scan width of 0.3°. A total of 606 frames per set were collected by using SMART[15] in three different settings of ϕ (0, 90, and 180°) keeping a sample-to-detector distance of 6.062 cm and a 2θ value fixed at –28°. The data were reduced by SAINTPLUS;[15] an empirical absorption correction was applied by using the package SADABS,[16] and XPREP[15] was used to determine the space group. The crystal structures were solved by direct methods with the use of SIR92[17] and refined by full-matrix least-squares methods with SHELXL97.[18] Molecular and packing diagrams were generated by using ORTEP32,[19] CAMERON,[20] and MERCURY.[21] The geometric calculations were done by PARST[22] and PLATON.[23] All hydrogen atoms were initially located in a difference Fourier map. The methine (CH) and methylene (CH_2) H atoms were then placed in geometrically idealized positions and allowed to ride on their parent atoms with C–H distances in the range 0.97–0.98 Å and U_{iso}(H) = 1.2U_{eq}(C). The OH hydrogen atoms were constrained to an ideal geometry with O–H distances fixed at 0.82 Å and U_{iso}(H) = 1.5U_{eq}(O). During refinement, each hydroxy group was, however, allowed to rotate freely about its C–O bond. The positions of the H atoms of the water molecule in the hemihydrate of hexol **4** were refined freely, along with an isotropic displacement parameter (Table 4). CCDC-688248 (hexol **3**), -688249 (hexol **4**), and -688250 (hexol **5**) contain the supplementary crystallographic data for this paper. These data can be obtained free of charge from The Cambridge Crystallographic Data Centre via www.ccdc.cam.ac.uk/data_request/cif.

Table 4. Summary of crystal data, data collection, structure solution, and refinement details.

	3	**4**	**5**
Formula	$C_{10}H_{18}O_6$	$2(C_{10}H_{18}O_6)\cdot H_2O$	$C_{10}H_{18}O_6$
M_r	234.24	486.50	234.24
Crystal size [mm]	0.31, 0.23, 0.21	0.20, 0.17, 0.16	0.39, 0.32, 0.25
Crystal system	orthorhombic	monoclinic	monoclinic
Space group	$P2_12_12_1$	$P2_1/n$	$P2_1/n$
a [Å]	9.279(3)	22.278(5)	6.520(2)
b [Å]	11.439(3)	6.5821(14)	38.751(13)
c [Å]	20.199(6)	15.698(3)	8.715(3)
α [°]	90	90	90
β [°]	90	111.356(4)	107.640(6)
γ [°]	90	90	90
V [Å^3]	2143.9(10)	2143.8(8)	2098.3(12)
Z	8	4	8
F (000)	1008	1048	1008
$\rho_{calcd.}$ [g cm^{-3}]	1.451	1.507	1.483
μ [mm^{-1}]	0.120	0.126	0.122
Reflns. collected	15767	8258	15666
l.s. Parameters	301	160	301
Unique reflns	2240	2186	3877
Observed reflns	1960	1634	2602
Index range	$-11 \le h \le 11$ $-13 \le k \le 13$ $-24 \le l \le 23$	$-27 \le h \le 27$ $-8 \le k \le 8$ $-18 \le l \le 19$	$-7 \le h \le 7$ $-46 \le k \le 43$ $-10 \le l \le 9$
R_1 [$I > 2\sigma(I)$]	0.0362	0.0645	0.0514
wR_2 [$I > 2\sigma(I)$]	0.0813	0.1555	0.1061
Goodness of fit	1.086	1.013	1.022
$\Delta\rho_{max/min}$ [e Å^{-3}]	0.189/–0.161	0.220/–0.239	0.291/–0.221

Supporting Information (see footnote on the first page of this article): ^{1}H and ^{13}C NMR spectra of hexols **3** and **5**.

Acknowledgments

We thank the Department of Science and Technology (DST), India for the CCD facility at the Indian Institute of Science (IISc), Bangalore. We sincerely acknowledge Prof. K. Venkatesan for his critical comments and helpful advice in preparing the manuscript. G. M. thanks the Council for Scientific and Industrial Research (CSIR), India for research support and the award of the Bhatnagar Fellowship.

[1] a) G. A. Jeffrey, W. Saenger in *Hydrogen Bonding in Biological Structures*, Springer, Berlin, **1991**; b) G. A. Jeffrey in *An Introduction to Hydrogen Bonding*, Oxford University Press, Oxford, UK, **1997**; c) G. A. Jeffrey, *Acta Crystallogr., Sect. B: Struct. Sci.* **1990**, *46*, 89–103.

[2] a) G. Mehta, S. Sen, K. Venkatesan, *CrystEngComm* **2005**, *7*, 398–401; b) G. Mehta, S. Sen, S. S. Ramesh, *CrystEngComm* **2005**, *7*, 563 –568; c) G. Mehta, S. Sen, *CrystEngComm* **2005**, *7*, 656–663; d) G. Mehta, S. Sen, S. S. Ramesh, *Eur. J. Org. Chem.* **2007**, 423–436; e) G. Mehta, S. Sen, K. Venkatesan, *CrystEngComm* **2007**, *9*, 144–151.

[3] Molecules possessing a center of symmetry usually crystallize in centrosymmetric space groups and tend to occupy a crystallographic inversion center, see: C. P. Brock, J. D. Dunitz, *Chem. Mater.* **1994**, *6*, 1118–1127.

[4] A. Shani, F. Sondheimer, *J. Am. Chem. Soc.* **1967**, *89*, 6310–6317.

[5] a) The quantity of hexol **4** obtained during the crystallization of its sibling **3** was estimated from the size and calculated density of the crystal obtained for the polycyclitol; b) see Supporting Information for ^{1}H and ^{13}C NMR spectra of hexols **3** and **5**.

[6] G. Mehta, S. S. Ramesh, *Tetrahedron Lett.* **2003**, *44*, 3105–3108.

[7] Due to the absence of any significant anomalous scatterers (Z > Si), attempts to confirm the absolute structure by refinement of the Flack parameter led to an inconclusive value of 0.3 (10) (see ref.[8]). Therefore, the intensities of the Friedel pairs (1668) were averaged prior to merging of data in $P2_12_12_1$ and the absolute configuration was assigned arbitrarily. The reported value of R_{int} corresponds to subsequent merging of equivalent reflections in this space group.

[8] a) H. D. Flack, *Acta Crystallogr., Sect. A: Found. Crystallogr.* **1983**, *39*, 876–888; b) H. D. Flack, G. Bernardinelli, *J. Appl. Crystallogr.* **2000**, *33*, 1143–1148.

[9] a) M. C. Etter, K.-S. Huang, *Chem. Mater.* **1992**, *4*, 824–827; b) S. George, A. Nangia, C.-K. Lam, T. C. W. Mak, J.-F. Nicoud, *Chem. Commun.* **2004**, 1202–1203; c) M. S. Hendi, P. Hooter, R. E. Davis, V. M. Lynch, K. A. Wheeler, *Cryst. Growth Des.* **2004**, *4*, 95–101.

[10] For recent references on γ-glycine, see: a) I. S. Lee, K. T. Kim, A. Y. Lee, A. S. Myerson, *Cryst. Growth Des.* **2008**, *8*, 108–113; b) S. K. Poornachary, P. S. Chow, R. B. H. Tan, *Cryst. Growth Des.* **2008**, *8*, 179–185; c) Z. Liu, L. Zhong, P. Ying, Z. Feng, C. Li, *Biophys. Chem.* **2008**, *132*, 18–22; d) J. W. Chew, S. N. Black, P. S. Chow, R. B. H. Tan, K. J. Carpenter, *CrystEngComm* **2007**, *9*, 128–130; e) K. Ambujam, S. Selvakumar, D. P. Anand, G. Mohamed, P. Sagayaraj, *Cryst. Res. Technol.* **2006**, *41*, 671–677.

[11] For further examples, see: a) I. Azumaya, D. Uchida, T. Kato, A. Yokoyama, A. Tanatani, H. Takayanagi, T. Yokozawa, *Angew. Chem. Int. Ed.* **2004**, *43*, 1360–1363; *Angew. Chem.* **2004**, *116*, 1384–1387; b) R. G. Gonnade, M. Bhadbhade, M. S. Shashidhar, *Chem. Commun.* **2004**, 2530–2531.

[12] E. Pidcock, *Chem. Commun.* **2005**, 3457–3459.

[13] C. P. Brock, *Acta Crystallogr., Sect. B: Struct. Sci.* **2002**, *58*, 1025–1031.

[14] a) T. Steiner, *Acta Crystallogr., Sect. B: Struct. Sci.* **2000**, *56*, 673–676; b) G. S. Nichol, W. Clegg, *CrystEngComm* **2007**, *9*, 959–960 and references cited therein; c) A. D. Bond, *CrystEngComm* **2008**, *10*, 411–415; d) A. Gavezzotti, *CrystEngComm* **2008**, *10*, 389–398.

[15] *SMART* (Version 6.028), *SAINT* (Version 6.02), *XPREP*, Bruker AXS Inc. Madison, Wisconsin, USA, **1998**.

[16] G. M. Sheldrick, *SADABS*, University of Göttingen, Germany, **1996**.

[17] A. Altomare, G. Cascarano, C. Giacovazzo, A. Guagliardi, M. C. Burla, G. Polidori, M. Camalli, *J. Appl. Crystallogr.* **1994**, *27*, 435.

[18] G. M. Sheldrick, *SHELXL97*, University of Göttingen, Germany, **1997**.

[19] L. J. Farrugia, *J. Appl. Crystallogr.* **1997**, *30*, 565.

[20] D. M. Watkin, L. Pearce, C. K. Prout, *CAMERON – A Molecular Graphics Package*, Chemical Crystallography Laboratory, University of Oxford, **1993**.

[21] a) I. J. Bruno, J. C. Cole, P. R. Edgington, M. K. Kessler, C. F. Macrae, P. McCabe, J. Pearson, R. Taylor, *Acta Crystallogr., Sect. B: Struct. Sci.* **2002**, *58*, 389–397; b) C. F. Macrae, P. R. Edgington, P. McCabe, E. Pidcock, G. P. Shields, R. Taylor, M. Towler, J. van de Streek, *J. Appl. Crystallogr.* **2006**, *39*, 453.

[22] M. Nardelli, *J. Appl. Crystallogr.* **1995**, *28*, 659.

[23] A. L. Spek, *J. Appl. Crystallogr.* **2003**, *36*, 7.

Received: September 15, 2008
Published Online: November 27, 2008

